JOURNAL OF AIRCRAFT
Vol. 46, No. 2, March–April 2009

F-16XL Geometry and Computational Grids Used in Cranked-Arrow Wing Aerodynamics Project International

O. J. Boelens*
National Aerospace Laboratory/NLR, 1006 BM Amsterdam, The Netherlands
K. J. Badcock†
University of Liverpool, Liverpool, England L69 7BZ United Kingdom
S. Görtz‡
Royal Institute of Technology, 100 44 Stockholm, Sweden
S. Morton§
U.S. Air Force, Eglin Air Force Base, Florida 32542
W. Fritz¶
European Aeronautic Defence and Space Company, 81633 Munich, Germany
S. L. Karman Jr**
University of Tennessee at Chattanooga, Chattanooga, Tennessee 37403
T. Michal††
The Boeing Company, St. Louis, Missouri 63166-0516
and
J. E. Lamar‡‡
NASA Langley Research Center, Hampton, Virginia 23681-2199

DOI: 10.2514/1.34852

The objective of the Cranked-Arrow Wing Aerodynamics Project International was to allow a comprehensive validation of computational fluid dynamics methods against the Cranked-Arrow Wing Aerodynamics Project flight database. A major part of this work involved the generation of high-quality computational grids. Before the grid generation, an airtight geometry of the F-16XL aircraft was generated by a cooperation of the Cranked-Arrow Wing Aerodynamics Project International partners. Based on this geometry description, both structured and unstructured grids have been generated. The baseline structured (multiblock) grid (and a family of derived grids) has been generated by the National Aerospace Laboratory. Although the algorithms used by the National Aerospace Laboratory had become available just before the Cranked-Arrow Wing Aerodynamics Project International and thus only a limited experience with their application to such a complex configuration had been gained, a grid of good quality was generated well within four weeks. This time compared favorably with that required to produce the unstructured grids in the Cranked-Arrow Wing Aerodynamics Project International. The baseline all-tetrahedral and hybrid unstructured grids have been generated at NASA Langley Research Center and the U.S. Air Force Academy, respectively. To provide more geometrical resolution, trimmed unstructured grids have been generated at the European Aeronautic Defence and Space Company's Military Air Systems, University of Tennessee at Chattanooga SimCenter, Boeing Phantom Works, Royal Institute of Technology, and the Swedish Defence Research Agency. All grids generated within the framework of the Cranked-Arrow Wing Aerodynamics Project International will be discussed in the paper. Both results obtained on the structured grids and the unstructured grids showed a significant improvement in agreement with flight-test data in comparison with those obtained on the structured multiblock grid used during the Cranked-Arrow Wing Aerodynamics Project.

Presented as Paper 488 at the 45th AIAA Aerospace Sciences Meeting and Exhibit, Reno, NV, 8–11 January 2007; received 28 September 2007; revision received 7 February 2008; accepted for publication 3 March 2008.

*Research and Development Engineer, Applied Computational Fluid Dynamics, Department of Flight Physics and Loads, Aerospace Vehicles Division, P.O. Box 90502; boelens@nlr.nl.
†Professor, Department of Engineering, Computational Fluid Dynamics Laboratory; K.J.Badcock@liverpool.ac.uk.
‡Research Scientist; currently DLR, German Aerospace Center, Lilienthalplatz 7, 38108 Braunschweig, Germany; Stefan.Goertz@dlr.de.
§Senior Research Scientist, Seek Eagle Office, 205 West D Avenue, Suite 346; Scott.Morton@eglin.af.mil.
¶Research and Development Engineer, Aerodynamics and Methods, Unit OPEA31; willy.fritz@eads.com.
**Research Professor, Graduate School of Computational Engineering; Steve-Karman@utc.edu.
††Technical Fellow; todd.r.michal@boeing.com.
‡‡Cranked-Arrow Wing Aerodynamics Project Principal Investigator, Configuration Aerodynamics Branch, Mail Stop 499; johnelamar@verizon.net.

Nomenclature

c_r	=	reference wing chord (24.7 ft or 328.8 in.)
$x_{\min}$, $x_{\max}$	=	minimum and maximum extent of the grid in the x direction, in.
$y_{\min}$, $y_{\max}$	=	minimum and maximum extent of the grid in the y direction, in.
y^+	=	Reynolds-number-like term for the flat-plate turbulent boundary layer
$z_{\min}$, $z_{\max}$	=	minimum and maximum extent of the grid in the z direction, in.
Δs_1	=	first normal distance from the wall, in.
$\Delta s_2/\Delta s_1$	=	viscous-grid-layer geometric progression parameter

I. Introduction

THE Cranked-Arrow Wing Aerodynamics Project (CAWAP) provides the computational fluid dynamics (CFD) community with an excellent database for validation and evaluation purposes [1]. The focus of this project was the understanding of the flow phenomena encountered on a cranked-arrow wing relevant to advanced fighter and transport aircraft. The subject of investigation was the F-16XL aircraft [2].

The Cranked-Arrow Wing Aerodynamics Project International (CAWAPI) [2], which was initiated by NASA, was a follow-up project to the Cranked-Arrow Wing Aerodynamics Project. Along with the Vortex Flow Experiment 2 [3], CAWAPI was incorporated under the NATO Research and Technology Organization's Applied Vehicle Technology task group AVT-113. The objective of the CAWAPI was to allow a comprehensive validation and evaluation of CFD methods against the CAWAP flight database [1].

Part of the work performed within CAWAPI involved the generation of high-quality computational grids. To allow high-quality grid generation, the available CAD geometry description of the F-16XL aircraft has been scrutinized. Issues encountered during this process are discussed in Sec. II.

At the beginning of the project, the task group members recognized the need to use common grids around this complex geometry to eliminate most of the uncertainties related to grid. The original plan was to have two common grids, one structured (multiblock) and one unstructured (tetrahedral). However, whereas all partners using structured CFD methods performed their simulation on a common structured multiblock grid generated at the National Aerospace Laboratory (NLR) (Sec. III), most partners using unstructured CFD methods have generated their own unstructured grid during the course of the project or have adapted existing grids (Sec. IV). A section with conclusions completes the paper.

The present paper only describes the generation of the high-quality computational grids (see also Table 1). The results obtained on both the structured and unstructured grids are described and discussed in the other papers in this special section of the *Journal of Aircraft* [2,4–7].

II. Geometry Description

The F-16XL airplane [1] is a single-place fighter-type prototype aircraft. The F-16XL airplane has a cranked-arrow wing with a leading-edge sweep angle of 70 deg inboard and 50 deg outboard of the crank. During all CAWAP flight tests, the aircraft was equipped with an air dam upstream of the actuator pod and wing-tip missiles. The airplane is shown in Fig. 1. For more details on the F-16XL airplane, see [1,2].

In the framework of the Cranked-Arrow Wing Project International project, the geometry of the F-16XL aircraft has been reconstructed using two surface descriptions, one from Lockheed Martin Aeronautics Company and one from NASA Langley Research Center (LaRC). The latter was obtained by measuring the actual aircraft in the NASA hangar, for which a numerical surface description was obtained through photogrammetric targets. This measurement was performed in the framework of the high-speed research program [1]. Using both surface descriptions and additional data for the inlet up to the compressor face and for the nozzle up to the turbine face, an updated initial graphics exchange specification (IGES) file has been generated by Lockheed Martin Aeronautics Company. It should be noted that for the configuration used, the control surfaces were not deflected. The updated IGES file contained a better characterization of the actual aircraft surfaces and leading edges, but was still not suitable for further grid generation purposes, because the geometry description contained multiple overlaying surfaces. This has been corrected at European Aeronautic Defence and Space Company, Military Air Systems (EADS-MAS), where a single set of describing surfaces was generated. The resulting surface description also included some refinements in the wing leading-edge region to improve future grid generation in this region. It was recognized by the CAWAPI members that this surface description

Table 1 Overview of the baseline structured and unstructured grids employed during CAWAPI

Grid	Generated by	Grid generation tool	Grid described in section	Grid size	Boundary-layer settings	Results shown in references
Baseline structured	NLR	In-house-developed, part of NLR's ENFLOW flow simulation system	III	1903 blocks 14,750,720 grid cells 17,014,119 grid points	$\Delta s_1 = 7.9 \cdot 10^{-7} c_r$ $\Delta s_2/\Delta s_1 = 1.1$	[4,5]
Baseline all-tetrahedral unstructured	NASA LaRC	GridTool, VGRIDns	IV.A	2,534,132 nodes 14,802,429 tetrahedra	——	[5,6]
Baseline hybrid unstructured	USAFA	Blacksmith	IV.A	2,535,842 nodes 1,442,394 prisms (9 layers) 10,482,709 tetrahedra	$\Delta s_1 = 6.6 \cdot 10^{-6} c_r$ $\Delta s_2/\Delta s_1 = 1.2$	[5,6]
EADS trimmed hybrid unstructured	EADS-MAS	CentaurSoft, adaptation algorithm in DLR-TAU code	IV.B.1	10,496,522 nodes $\sim 15,600,000$ prisms (29 layers) $\sim 13,500,000$ tetrahedra	$\Delta s_1 = 4.8 \cdot 10^{-7} c_r$ $\Delta s_2/\Delta s_1 = 1.3$	[5,7]
UTSimCenter trimmed hybrid unstructured	UTSimCenter	Gridgen, in-house-developed	IV.B.2	13,906,708 nodes 15,770,674 prisms (25 layers) 166,230 pyramids, 32,395,936 tetrahedra	$y^+ \sim 1$ $\Delta s_2/\Delta s_1 = 1.15$ Geometric growth rate is 1.02	[5,7]
Boeing trimmed hybrid unstructured	Boeing Phantom Works	MADCAP, AFLR	IV.B.3	$\sim 19,300,000$ cells 15 prismatic layers	$\Delta s_1 = 9.1 \cdot 10^{-7} c_r$ $\Delta s_2/\Delta s_1 = 1.2$	[5,7]

Fig. 1 F-16XL aircraft.

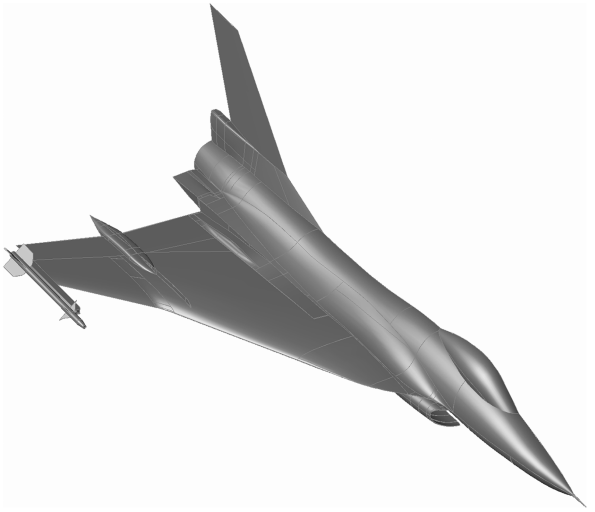

Fig. 2 Airtight geometry of the F-16XL aircraft.

still needed some further modifications to facilitate the generation of a structured grid. The following modifications have been applied:

1) The gap between the launcher and the missile was closed. Other details of the missile, such as the fins, were unmodified.

2) The gap between the nozzle and the trailing-edge flap was closed.

3) The environmental control system inlet was simplified.

4) A step in the longitudinal progression of the nose-boom outer diameter was smoothed out.

These modifications were made at LaRC. Finally, the modified surface description has been checked for airtightness and corrected by EADS-MAS, when necessary, using the commercial CAD tool CADfix. This IGES file containing the airtight geometry description (see Fig. 2) has been used for both the structured and unstructured grid generation.

III. Structured Multiblock Grid

A. Background

During CAWAP, a structured multiblock grid had been generated at LaRC [1,2]. This grid was based on a previous IGES file and exhibited an average y^+ value of 82 at a flight Reynolds number of around 40×10^6. Simulations on this grid [2] were performed using the wall-function option in the turbulence model. Because none of the participants of CAWAPI employed such a wall-function option in the turbulence model, it was decided that for CAWAPI purposes, a new structured multiblock grid had to be generated. The plan, as detailed in [8], was for "two members of the CAWAPI—one at NLR and the other at the University of Glasgow (UGlasgow)" to

> collaborate in the development of the structured grid for their own use as well as for others. This is a risky endeavor even if the developers are colocated or on the same hall, but certainly more so if they are in two different countries and having to rely on the virtual laboratory (VL) for all grid exchanges. The plan was for the NLR to produce the blocking strategy with implementation and for UGlasgow to adjust the grid spacing, as needed. Alternatively, NLR could produce and test the grid then UGlasgow would perform a second test on the grid before its general release to the facet. In either case, both would use and support the same grid file. For this problem, it turned out that the alternate plan was the one implemented due, in part, to the difficulties experienced with the transfer of large files. . .from this newly developed VL.

B. Grid Generation Algorithm

The structured multiblock grid has been generated at the NLR using a Cartesian grid mapping technique. The (semi-automatic) grid generation algorithms have been developed at NLR and are part of NLR's ENFLOW flow simulation system [9]. Most of these algorithms had become available just before CAWAPI and had only been applied to a clean (no external loads) F-16 configuration. Being the first realistic case to which these tools were applied and bearing in mind that a limited experience with their use existed, it was estimated that six weeks would be needed to generate a complete structured multiblock grid around the half-span full-scale model of the F-16XL aircraft.

The Cartesian grid generation technique used by the NLR can be subdivided into the following steps:

1) Imagine/construct a Cartesian abstraction of the geometry description. In such an abstraction, the geometry (including all details) is represented by a set of Cartesian blocks. The abstraction of the half-span full-scale model of the F-16XL used in CAWAPI is shown in Fig. 3. In this figure, it can be observed that each fin of the wing-tip missile, for example, is represented by a single block. Note furthermore that the engine duct and the nozzle have been closed in this abstraction.

2) Project the abstraction onto the real geometry description. The projected abstraction of the half-span full-scale model of the F-16XL is shown in Fig. 4.

3) Generate the so-called Navier–Stokes blocks. This first layer of blocks around the geometry, including the engine duct and the nozzle, is generated by a simple blowup technique. The surface patches are translated along the outward normal to the geometry using the corners of the patches as control points. The algorithm uses accounts for symmetry planes and only needs the offset of the blocks as input. The generated layer of blocks has an O-O-type topology. During this step, the blocks to fill up the engine duct and the nozzle are also inserted interactively.

4) Generate the field blocks in the Cartesian space. The faces of the Navier–Stokes blocks opposite to the geometry combined with the faces at the engine duct inlet and nozzle exit display the same Cartesian structure as the abstraction shown in Fig. 3. In the Cartesian space, the field blocks are generated automatically. As is evident from Fig. 3, the blocks in the Cartesian space are simple cubical blocks.

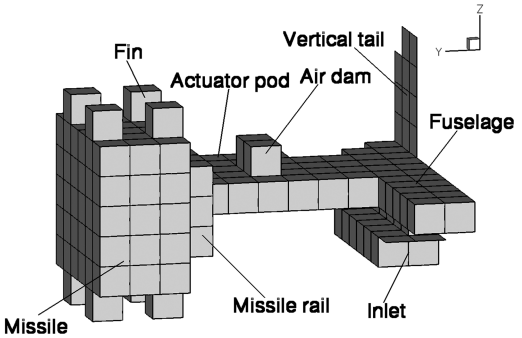

Fig. 3 Abstraction of the surface geometry for the half-span model of the F-16XL.

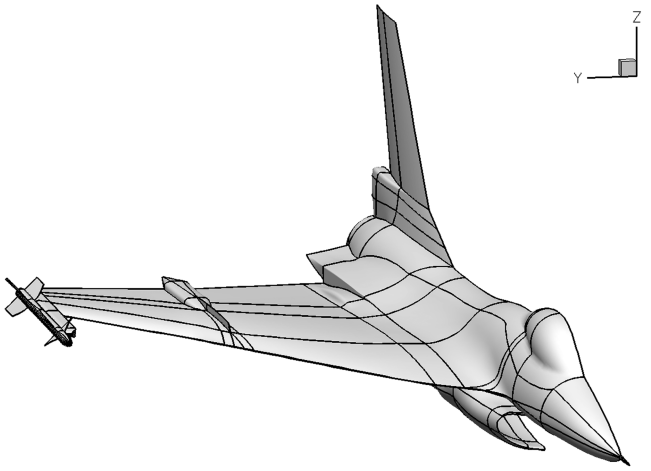

Fig. 4 Projected abstraction for the half-span model of the F-16XL.

5) Generate the field blocks in the physical space. The simple cubical blocks in the Cartesian space are automatically mapped to the physical space using a grid deformation technique [10]. The algorithm accounts for symmetry planes. Finally, the so-called far-field blocks are added to the topology interactively. The far-field boundaries are located several reference wing chords away from the model.

6) Set the (Euler) grid dimensions. Each edge is assigned a grid dimension. The minimum number of cells used along an edge is eight, to ensure three levels of multigrid. In the Navier–Stokes blocks, eight cells were used in the surface normal direction.

7) Automatically connect the edges. The grid spacing in the grid is set automatically. For each set of adjoining edges, the grid point density is adjusted such that a smooth transition of the grid is obtained. In general, this means that the grid point density of the edge with the larger grid spacing is linked to that of the edge with the smaller grid spacing.

8) Improve the grid quality by an elliptical smoothing algorithm. An elliptical smoothing algorithm is applied to the grid. As a result of this algorithm, the quality in terms of grid smoothness is improved significantly.

9) Increase the resolution in the Navier–Stokes blocks. To provide for sufficient boundary-layer resolution, the number of grid points in the surface normal direction in the Navier–Stokes blocks is increased. In addition, a redistribution of the grid points with a specified stretching away from the geometry is applied. The algorithm used accounts for a smooth transition to the grid in the outer blocks.

Within NLR's ENFLOW flow simulation system [9], further algorithms exist to do the following:

1) Merge blocks within a grid to reduce the total number of blocks.

2) Mirror a grid with respect to a symmetry plane to obtain a full-configuration grid from a half-configuration grid.

3) Convert the grid from NLR's native ENFLOW format to several other formats, such as Plot3D or CFD General Notation System (CGNS) [11].

The characteristics of the structured grid obtained using this Cartesian grid mapping technique are described in the next section. Instead of the six weeks estimated before the project, the structured grid has been generated well within four weeks, including some further development of the grid generation algorithms.

C. Characteristics of the Structured Multiblock Grid

During the grid generation process, the following modifications to the surface description of the F-16XL aircraft have been made to further facilitate the generation of a multiblock structured grid:

1) A small step or plate on the wing upper surface was removed.

2) The end part of the vertical tail base was slightly rounded off.

It is expected that these modifications do not influence the simulated flow significantly.

The following family of structured grids has been used in CAWAPI:

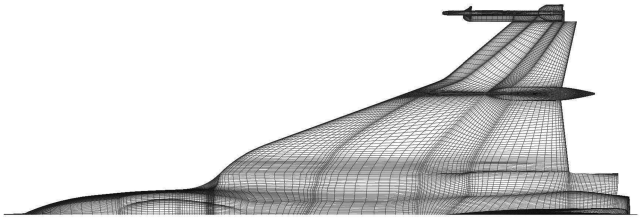

Fig. 5 Upper-surface grid for the structured multiblock grid for the half-span model of the F-16XL.

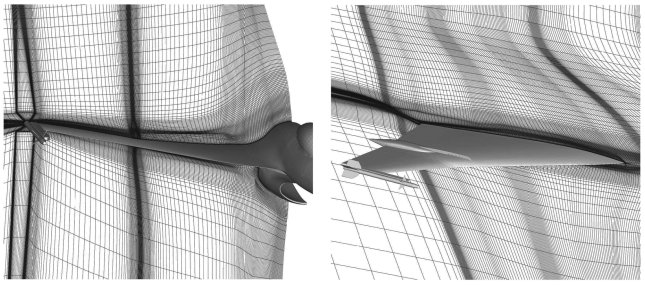

a) **b)**

Fig. 6 Grid planes showing the grid density of the aircraft surface in a) a plane approximately normal to the flow direction (the fuselage station is constant) and b) a plane approximately parallel to the flow direction (the butt line is constant).

1) A baseline structured grid around the half-span full-scale model of the F-16XL consisting of 1903 blocks, 14,750,720 grid cells, and 17,014,119 grid points has been generated.

2) A baseline structured grid with the far-field blocks divided into smaller blocks so that only a one-to-one connection between block faces exists has been generated. This version was used by the University of Liverpool.

3) A baseline structured grid with a reduced number of blocks has been generated. The first merging step was performed at NLR, reducing the number of blocks from 1903 to 216. A further small reduction was accomplished at LaRC that yielded a grid with only 200 blocks.

4) A structured grid around the full-scale model of the F-16XL consisting of 3806 blocks, 29,501,440 grid cells, and 34,028,238 grid points has been generated. This grid has been generated by mirroring the baseline structured grid around the half-span full-scale model of the F-16XL with respect to the symmetry plane. This grid has only been used by NLR.

Some further details of the baseline structured grid around the half-span full-scale model of the F-16XL are summarized in Table 1.

The upper-surface grid of the structured multiblock grid is shown in Fig. 5. In Fig. 6, the grid is shown in both a plane approximately normal to the flow direction (the fuselage station is constant) and a plane approximately parallel to the flow direction (the butt line is constant).

A good resolution of the boundary layer requires the grid to be clustered in the direction normal to the surface with the spacing of the first grid point off the wall to be well within the laminar sublayer of the boundary layer. For turbulent flows, the first point off the wall should exhibit a y^+ value of approximately one. The resulting y^+ distribution over the upper surface for the structured multiblock grid is shown in Fig. 7 for flight condition 19. From this figure, it is evident that the grid spacing normal to the surface results in y^+ values of approximately one.

The grid converted to Plot3D format was uploaded to the VL [2,8] at LaRC to be used by other researchers in CAWAPI.

IV. Unstructured Grids

During CAWAP, no unstructured grid had been generated. Within the framework of CAWAPI, the plan was to generate a common

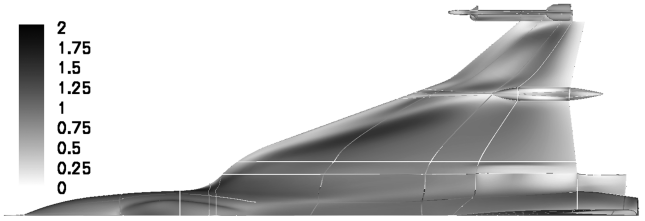

Fig. 7 Levels of y^+ on the upper surface for the structured multiblock grid for flight condition 19 ($\alpha = 11.85$ deg, $M = 0.360$, and $Re = 46.80 \times 10^6$). Results are obtained using the turbulent/non-turbulent k-ω turbulence model with correction for vortical flows.

unstructured (tetrahedral) grid. However, as discussed in Sec. I, most partners using unstructured CFD methods have generated their own unstructured grid during the course of CAWAPI or have adapted existing grids (see Table 1). Baseline all-tetrahedral and hybrid unstructured grids (Sec. IV.A) have been generated at LaRC and the U.S. Air Force Academy (USAFA), respectively. Trimmed unstructured grids have been generated at EADS-MAS (Sec. IV.B.1), the UTSimCenter (Sec. IV.B.2), and Boeing Phantom Works (Sec. IV.B.3). In addition, a series of highly adapted grids, both Euler and Navier–Stokes, has been generated at the Swedish Royal Institute of Technology and Swedish Defence Research Agency (KTH/FOI). The grids that have been used in an extensive study of flight condition 70 are discussed in [5].

A. Baseline Unstructured Grids

At LaRC, a baseline unstructured all-tetrahedral viscous grid with 2,534,132 nodes, corresponding to 14,802,429 cells, has been generated around the half-span full-scale model of the F-16XL using the grid generation packages GridTool [12] and VGRIDns [13].

This grid has been converted to a hybrid baseline unstructured grid in Cobalt [14] format at USAFA using the commercial grid management utility Blacksmith from Cobalt Solutions, LLC. Blacksmith reduced the cell count to a total of 11,928,103, corresponding to 2,535,842 nodes, by combining highly stretched tetrahedral cells into prismatic cells. The program generated nine layers of prismatic cells, corresponding to 1,442,394 prisms. The reason the grid had only nine prismatic layers is that pyramids would be needed as end caps for layers that are not complete. Rather than adding another cell type, it was decided to accept those nine layers. The transition between the prismatic layers and the tetrahedral grid is very smooth. The surface of the half-span full-scale model of the F-16XL is discretized with 160,266 triangular elements. The upper-surface grid is shown in Fig. 8.

For the hybrid baseline unstructured grid, the spacing of the first grid point normal to the solid wall is $6.6 \times 10^{-6}\ c_r$. Away from the wall, the spacing increases by a ratio $\Delta s_2/\Delta s_1$ of 1.2. Inspection of the y^+ distribution over the upper surface of the aircraft model showed that the grid spacing normal to the surface led to an average y^+ value of 1 and a maximum y^+ value of about 2 under the primary wing vortex, demonstrating that the grid is fine enough at the wall boundaries.

The engine duct is meshed all the way to the compressor face, and the nozzle is meshed from the engine mixing plane (see Fig. 9). The grid density of the aircraft surface is shown in Fig. 10, which depicts a wrinkly cutting plane through the grid at FS496 (the fuselage station on the airplane in inches, positive aft), close to the trailing edge.

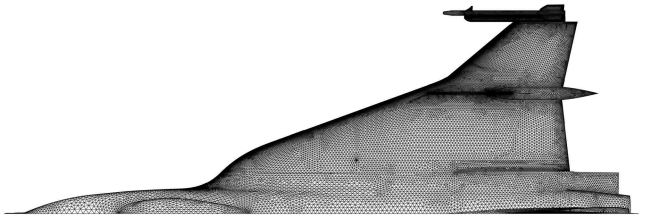

Fig. 8 Surface grid of the hybrid baseline unstructured grid for the half-span model of the F-16XL (160,266 faces).

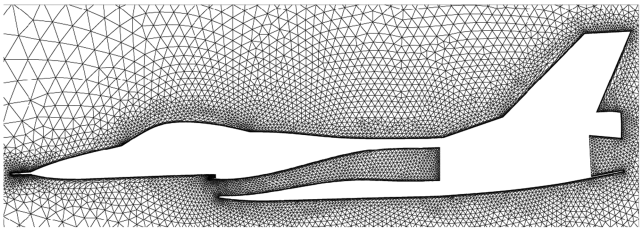

Fig. 9 Symmetry plane of the hybrid baseline unstructured grid showing the grid in the engine duct and nozzle.

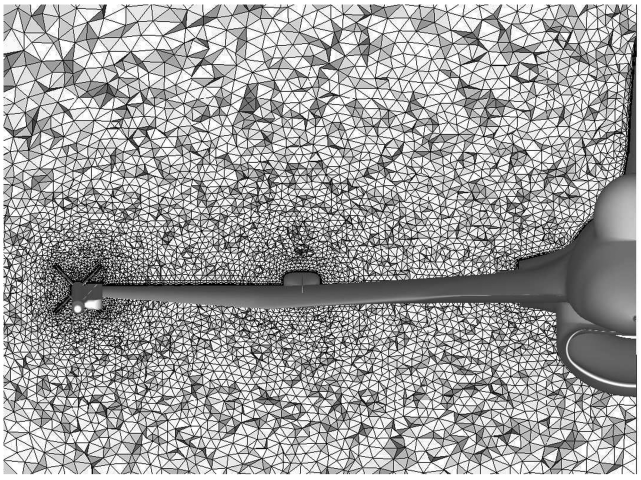

Fig. 10 Wrinkly cutting plane of the hybrid baseline unstructured grid at FS496 showing the grid density of the aircraft surface close to the trailing edge of the wing.

Next, researchers at KTH/FOI converted the hybrid grid from Cobalt format to the Flexible Format Architecture (FFA) [15], the native format of the Swedish CFD code EDGE [16]. In this conversion step, all grid dimensions were converted from inches to meters.

Finally, KTH/FOI researchers converted the FFA-format grid to the CGNS [11] library version 2.3. The resulting CGNS file was uploaded to the VL [2,8] at LaRC to be used by other researchers in CAWAPI.

B. Trimmed Unstructured Grids

1. EADS-MAS

At EADS-MAS, the grid adaptation technique, which is included in the DLR-TAU code [17], has been used for the CAWAPI CFD calculations. The starting point was an initial grid, which subsequently is adapted 4 times during the flow calculations. The initial grid has been generated using the commercial CentaurSoft grid generator, which enables the generation of hybrid grids with minimal user interaction. Starting from the airtight geometry description, the grid generation process is split up into surface triangulation, prismatic-grid generation, and tetrahedral-grid generation. Point clustering is achieved by automatic clustering based on geometric features and by user-controlled clustering placing so-called sources. This user-controlled clustering has been used for a rough adaptation of the grid to the expected vortical flow structure. The surface triangulation works in a patch-oriented way, which results in a high resolution of all small surface patches. This high resolution, however, is not always needed. The geometry description of the F-16XL aircraft contains several such minipatches. Because the adaptation algorithm of the DLR-TAU code uses the surface grid as a geometry base, the surface triangulation of this initial grid was already relatively fine to ensure a sufficient resolution of all geometric details. The tetrahedral grid, however, was kept somewhat coarse and was expected to be refined by the adaptation.

The resulting initial grid is a hybrid grid with 10,496,522 nodes in total for the half-span full-scale model of the F-16XL. It has a prismatic layer of 15.6 million prisms in the near-wall region and 13.5 million tetrahedra in the outer region. The thickness of the first prismatic layer is 4.8×10^{-7} c_r, and a geometric progression parameter $\Delta s_2/\Delta s_1$ of 1.3 is used for the other 29 viscous layers. In critical regions the prismatic layers are chopped, and transition elements such as pyramids and tetrahedra are created. The surface of the aircraft is resolved by 749,742 triangles.

This grid has been used as the initial grid for all symmetric flight conditions. During the calculations, it has been adapted in four steps for each flight condition. In the adaptation feature of the DLR-TAU code, the edges of the primary grid are bisected, depending on a refinement sensor. The refinement sensor is based on the differences of the flow variables: velocity, density, total pressure, and helicity. During the adaptation process, points can be added and removed. The structure of the initial grid, however, is maintained, because only points added to this grid can be removed. The adaptation algorithm can be started after the computation of a flow solution on a certain grid. It then generates a new grid and interpolates the solution onto this grid. The maximum increase of grid points for each of the four adaptation steps was limited to 25%. Grid points have been added in the surface grid and in the tetrahedral grid. The new surface points have been included in the prismatic grid; however, the number of the prismatic layers and their thicknesses have not been changed. The initial prismatic layer was designed such that it was suitable for a much finer grid.

Using this adaptation procedure, a final adapted grid has been obtained for each flight condition. For example, for flight condition 25 the final adapted grid consists of 1,462,096 surface triangles, 32,375,977 prisms, and 25,871,331 tetrahedra. Compared with the initial grid, the number of surface triangles, prisms, and tetrahedra has been roughly doubled, resulting in a total number of 21,149,945 nodes. Figure 11 shows a comparison of the initial grid and the final adapted surface grid for flight condition 25. New grid points mainly have been added along the leading edge (due to the leading-edge suction), inboard and outboard of the suction peak of the primary vortex (due to the pressure gradients) and in the tip section of the outer wing. In space, new points have been added in regions with vortical flow above the wing and in the wake region behind the wing.

2. *University of Tennessee at Chattanooga SimCenter*

One of the more unique grid systems has been produced by researchers at the University of Tennessee at Chattanooga SimCenter (UTSimCenter). Two separate grid generation programs have been used to generate the viscous grids used by UTSimCenter within CAWAPI. The first program was a commercially available mesh generation package known as Gridgen. Gridgen was used to create an inviscid unstructured grid. The second grid generation program was developed in-house at the UTSimCenter and was used to insert viscous layers in the inviscid grid [18].

a. Inviscid Grid. Gridgen has been used to create an unstructured inviscid grid, composed of mostly tetrahedra. A surface grid, consisting of triangular elements, was generated on the airtight geometry description. Care was taken to ensure proper resolution of pertinent geometric features such as the leading and trailing edges of the wing. The high curvature of the leading and trailing edges needed fine resolution in the chordwise direction to resolve the shape. The unstructured triangular surface meshing in Gridgen imposes nearly isometric triangular elements. To provide the desired resolution in the chordwise direction and not have an excessive number of elements in the spanwise direction, a structured grid was used along the leading and trailing edges of the wing. The aspect ratio of the quadrilateral elements was imposed to be no larger than 15. The resulting structured quadrilateral surface grid was then converted to an unstructured triangular grid by subdividing the quadrilateral elements into two triangles. Figure 12 shows a section of the leading edge on which the converted structured-mesh domain meets the unstructured-mesh domains. A view of the mesh on the symmetry plane is shown in Fig. 13.

Baffle surfaces were used to control the spacing of the volume grid, resulting in a hybrid unstructured inviscid grid. The quadrilateral elements shown in the figure around the nose and tail are a result of these baffles. Additional baffles were created around the leading edge and trailing edge of the wing and at a near-field boundary within a body length of the aircraft.

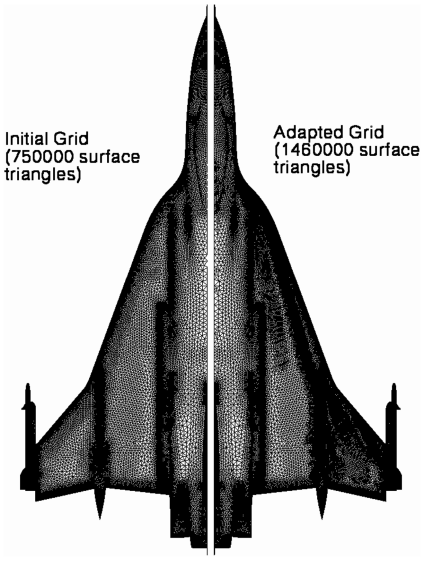

Fig. 11 Initial EADS-MAS surface grid and final adapted grid for flight condition 25 ($\alpha = 19.84\,\mathrm{deg}$, $M = 0.242$, and $Re = 32.22 \times 10^6$).

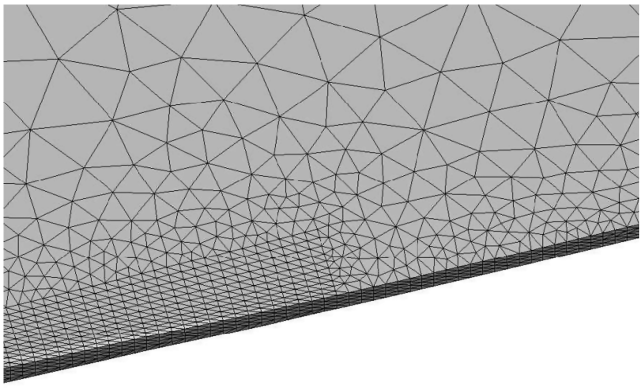

Fig. 12 Leading-edge grid showing the converted structured grid domain next to an unstructured grid domain.

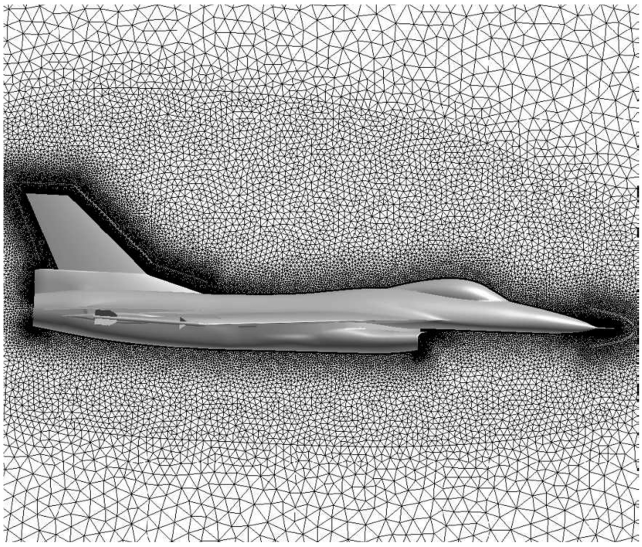

Fig. 13 Symmetry plane of the inviscid unstructured grid generated by UTSimCenter using Gridgen.

b. Viscous-Layer Addition. An in-house-developed grid generation program was used to insert layers of triangular prismatic elements at the no-slip surfaces of the geometry [18]. This method uses a linear–elastic grid smoothing scheme to push the existing grid away from the surface, making room for the viscous elements. The term normally used to define Young's modulus in the linear–elastic relations is defined using a combination of element aspect ratio and corner angles to provide stiffness in regions of tight grid spacing. Poisson's ratio was set to a constant of 0.25. Only one layer of points at a time is added in reverse order; the top layer is added first and the final layer near the wall is added last. Points are only added when the local mesh spacing is larger than the desired spacing for the current layer. As a result, the number of triangular prismatic elements in a column varies over the surface. Figures 14 and 15 show the varying number of elements per column for the grid at the inlet. This capability allows the outer layer of prisms to match the spacing of the local tetrahedral elements without forcing each column to have unnecessary layers, which could result in kinking or buckling of the outer viscous layers.

A total of 25 layers was requested for the viscous region. The initial spacing was specified to correspond to an approximate y^+ value of 1. The height of the subsequent layers increases according to a geometric progression parameter $\Delta s_2/\Delta s_1$ of 1.15 and a geometric growth rate of 1.02. A view of the viscous layers for the tip missile fins is shown in Fig. 16. Finer resolution tetrahedra can be seen in the gap region between the fin and the missile rail. The layer insertion strategy matched the normal spacing of the layers with the existing local tetrahedral grid. The viscous grid for the half-span model of the F-16XL contains 13,906,708 nodes, 32,395,936 tetrahedra, 166,230 pyramids, and 15,770,674 prisms.

3. Boeing Phantom Works

The grids used by researchers from the Boeing Phantom Works have been generated using the Boeing Modular Aerodynamic Computational Analysis Process (MADCAP), developed at Boeing as a modular framework to house grid generation capabilities from a variety of sources. MADCAP contains a fully automated surface grid generation capability. In addition to the automated approach, the user can interactively control resolution and grid element type through the selection of control nodes, edges, and surfaces. Unstructured grid generation algorithms can be selected from Boeing-developed libraries and/or from the Advancing Front with Local Reconnection (AFLR) library [19]. Surface grids can contain a combination of quadrilateral and triangular faces. The volume grids used in this study have been developed with the AFLR code using a combination of element types. Near the wall, advancing layers have been used to place highly anisotropic prismatic elements across the boundary layer. Outside the boundary layer, isotropic tetrahedral elements have been used.

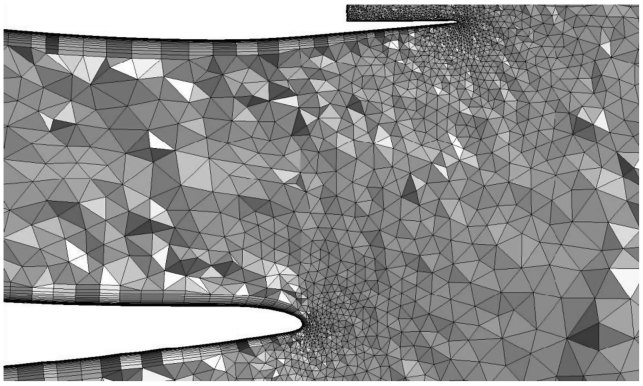

Fig. 14 Wrinkly cutting plane of the viscous unstructured grid generated by UTSimCenter near the symmetry plane at the inlet.

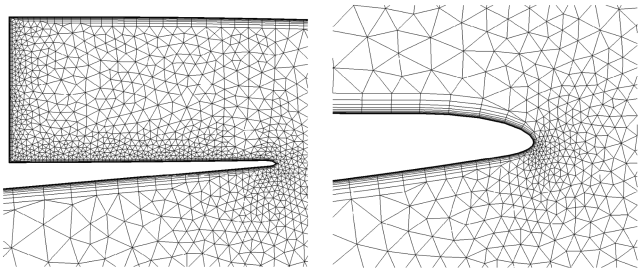

a) **b)**

Fig. 15 Magnified views of the grid on the symmetry plane of the viscous unstructured grid generated by UTSimCenter at the a) upper inlet lip and b) lower inlet lip.

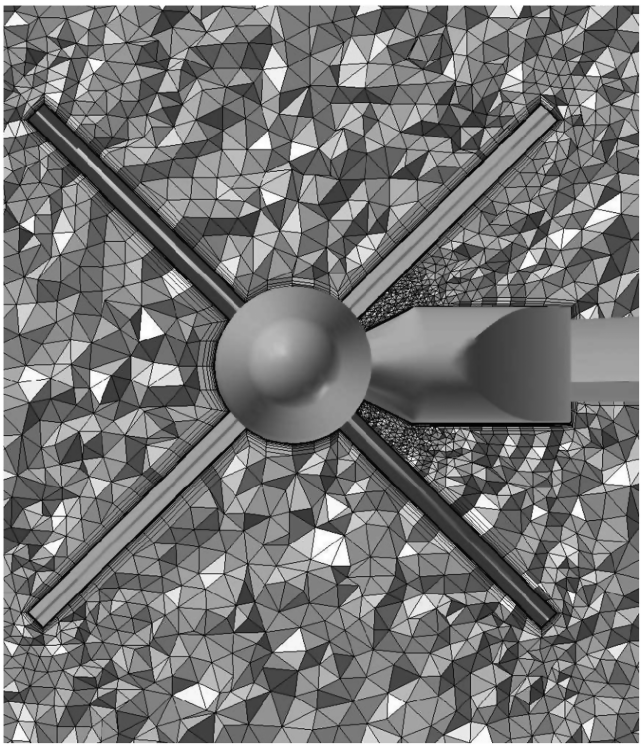

Fig. 16 Magnified view of an axial cut of the viscous unstructured grid generated by UTSimCenter through the tip missile fins and wing.

A smooth transition between the prismatic and tetrahedral elements is provided by growing each column of the boundary-layer grid until the element at the outside edge is nearly isotropic. The boundary-layer resolution is controlled by specification of the initial spacing near the wall, an initial growth rate, a growth stretching, and a maximum growth rate. In addition, the extent of the boundary-layer thickness can be specified or an estimate of the boundary-layer thickness for a turbulent flat plate can be used to extend the prismatic layers beyond the estimate. Control of the resolution of the tetrahedral portion of the grid is provided by a linear interpolation from the surface grid. Alternatively, the user can specify a geometry growth rate to control the stretching of resolution in the tetrahedral region. Sources in the form of individual nodes, curves, or surfaces can be specified to control the offbody resolution of the tetrahedral grid.

A grid with higher resolution than the hybrid baseline unstructured grid was constructed in MADCAP to try to improve solution accuracy. In particular, the grid was concentrated near the wing leading edge to try to improve the prediction near the secondary vortex. Grid resolution was increased at the leading edge by introducing high-aspect-ratio quadrilateral elements into the surface grid. The maximum aspect ratio of the quadrilateral faces is 25. The circumferential resolution at the leading edge is $1.5 \times 10^{-4}\ c_r$ inboard of the wing crank, transitioning to $3.0 \times 10^{-5}\ c_r$ spacing near the wing tip. The quadrilateral elements were subdivided into triangles in the final grid. A comparison of the Boeing and common hybrid baseline unstructured grid at the wing leading edge is shown in Fig. 17. The resolution of the Boeing surface grid is about double

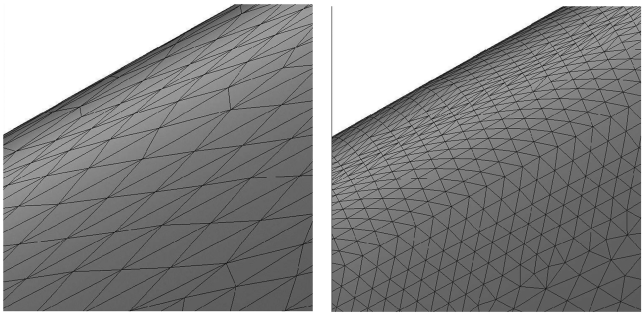

a) b)

Fig. 17 Comparison of surface grids near the wing leading edge: a) hybrid baseline unstructured grid and b) Boeing grid.

that of the common mesh in the immediate proximity of the wing vortices.

The volume portion of the Boeing grid was generated in AFLR and consists of a semistructured boundary-layer extrusion connected to an isotropic tetrahedral grid. The extrusion used a $9.1 \times 10^{-7}\ c_r$ initial spacing at the wall to yield a y^+ value of approximately 1. The initial spacing grew geometrically with an initial geometric progression parameter $\Delta s_2/\Delta s_1$ of 1.2, ending at a 1.8 maximum growth ratio. Extrusion terminated when the prisms achieved an aspect ratio near unity. The combination of the initial viscous spacing, growth rate parameters, and surface spacing produced approximately 15 prism layers. The resulting volume grid had 19.3 million cells.

The tetrahedral portion of the Boeing grid has been refined at flight conditions 7 and 25 using feature-based grid adaption.

V. Conclusions

In the framework of the Cranked-Arrow Wing Aerodynamics Project International (CAWAPI), both structured and unstructured grids have been generated (see Table 1). Before the grid generation, an IGES file containing the airtight geometry description of the half-span model of the F-16XL aircraft has been generated that could be used for both the structured and unstructured grid generation.

The baseline structured grid has been generated by NLR using in-house-developed (semi-automatic) grid generation algorithms. A family of grids, including grids with a reduced number of blocks, have been derived from this baseline grid. Although most of the algorithms used had become available just before CAWAPI and thus only limited experience had been gained with their application to a configuration as complex as the F-16XL aircraft, a grid of good quality was generated well within four weeks, including some further development of the grid generation algorithms. This time compared favorably with that required to produce the unstructured grids in CAWAPI. The best practices established during CAWAPI have resulted in a significant reduction of the structured grid generation time for future projects.

Several unstructured grids have been generated within CAWAPI. The baseline all-tetrahedral and hybrid unstructured grids have been generated at LaRC and USAFA, respectively. Despite their rather moderate cell count, the baseline all-tetrahedral and hybrid unstructured grids provided sufficient geometrical resolution. However, several CAWAPI members needed grids with more geometrical resolution. Trimmed unstructured grids have been generated at EADS-MAS, UTSimCenter, Boeing Phantom Works, and KTH/FOI.

Results obtained on both the structured grids and the unstructured grids showed a significant improvement in agreement with flight-test data in comparison with those obtained on the structured multiblock grid used during CAWAP [9]. The CAWAPI results obtained on the structured grids are described and discussed in [4,5], and the results obtained on the unstructured grids are detailed in [5–7].

Acknowledgments

Part of this work has been conducted under NLR's programmatic research funding. The authors gratefully acknowledge the support provided by Lockheed Martin Aeronautics Company in providing the refined initial graphics exchange specification (IGES) geometry file. In addition, the authors gratefully acknowledge the geometrical work performed by Edward B. Parlette of Vigyan, Inc., in generating unstructured grids from the IGES file.

References

[1] Lamar, J. E., Obara, C. J., Fisher, B. D, and Fisher, D. F., "Flight, Wind-Tunnel, and Computational Fluid Dynamics Comparison for Cranked Arrow Wing (F-16XL-1) at Subsonic and Transonic Speeds," NASA TP-2001-210629, 2001.

[2] Obara, C. J., and Lamar, J. E., "Overview of the Cranked-Arrow Wing Aerodynamics Project International," *Journal of Aircraft*, Vol. 46, No. 2, 2009, pp. 355–368. doi:10.2514/1.34957

[3] Hummel, D., and Redeker, G., "A New Vortex Flow Experiment for Computer Code Validation," *Advanced Flow Management, Part A: Vortex Flow and High Angle of Attack Papers on Disc* [CD-ROM], NATO Research and Technology Organization, Neuilly sur Seine, France, May 2001, Paper 8.

[4] Boelens, O. J., Badcock, K. J., Elmilgui, A., Abdol-Hamid, K. S., and Massey, S. J., "Comparison of Measured and Block Structured Simulations for the F-16XL Aircraft," *Journal of Aircraft*, Vol. 46, No. 2, 2009, pp. 377–384. doi:10.2514/1.35064

[5] Rizzi, A., Jirasek, A., Badcock, K. J., Lamar, J. E., Boelens, O. J., and Crippa, S., "What Was Learned from Numerical Simulations of F-16XL (CAWAPI) at Flight Conditions," *Journal of Aircraft*, Vol. 46, No. 2, 2009, pp. 423–441. doi:10.2514/1.35698

[6] Goertz, S., Jirasek, A., Morton, S. A., McDaniels, D. R., Cummings, R. M., Lamar, J. E., and Abdol-Hamid, K. S., "Standard Unstructured Grid Solutions for CAWAPI F-16XL," *Journal of Aircraft*, Vol. 46, No. 2, 2009, pp. 385–408. doi:10.2514/1.35163

[7] Fritz, W., Davis, M. B., Karman, S. L., Jr., and Michal, T., "RANS Solutions for the CAWAPI F-16XL Using Different Hybrid Grids," *Journal of Aircraft*, Vol. 46, No. 2, 2009, pp. 409–422. doi:10.2514/1.35106

[8] Lamar, J. E., Cronin, C. K., and Scott, L. E., "Virtual Laboratory Enabling Collaborative Research in Applied Vehicle Technologies," *Flow Induced Unsteady Loads and the Impact on Military Applications Papers on Disc* [CD-ROM], NATO Research and Technology Organization, Neuilly sur Seine, France, Apr. 2005.

[9] Boerstoel, J. W., Kassies, A., Kok, J. C., and Spekreijse. S. P., "ENFLOW, a Full-Functionality System of CFD Codes for Industrial Euler/Navier–Stokes Flow Computations," National Aerospace Lab., Rept. NLR TP 96286U, Amsterdam, 1996.

[10] Spekreijse, S. P., Prananta, B. B., and Kok, J. C., "A Simple, Robust and Fast Algorithm to Compute Deformations of Multiblock Structured Grids," National Aerospace Lab., Rept. NLR-TP-2002-105, Amsterdam, 2002.

[11] Legensky, S. M., Edwards D. E., Bush R. H., Poirier D. M. A., Rumsey, C. L., Cosner R. R., and Towne, C. E., "CFD General Notation System (CGNS): Status and Future Directions," AIAA Paper 2002-0752, 2002.

[12] Samareh, S., "GridTool: A Surface Modeling and Grid Generation Tool," NASA CP-3291, 1995.

[13] Pirzadeh, S., "Progress Toward a User-Oriented Unstructured Viscous Grid Generator," AIAA Paper 96-0031, 1996.

[14] Strang, W. Z., Tomaro, R. F., and Grismer, M. J., "The Defining Methods of Cobalt: A Parallel, Implicit, Unstructured Euler/Navier–Stokes Flow Solver," AIAA Paper 99-0786, 1999.

[15] Wallin, S., "Standardized Data Format," Aeronautical Research Inst. of Sweden, Rept. FFAP-A-950, Stockholm, 1992.

[16] Eliasson, P., "EDGE, a Navier–Stokes Solver for Unstructured Grids," *Finite Volumes for Complex Applications 3*, Hermes, Paris, 2002, pp. 527–534.

[17] Gerhold, T., Friedrich, O., Evans, J., and Galle, M., "Calculation of Complex Three-Dimensional Configurations Employing the DLR-TAU Code," AIAA Paper 97-0167, 1997.

[18] Karman, S., Jr., "Unstructured Viscous Layer Insertion Using Linear–Elastic Smoothing," AIAA Paper 2006-0531, 2006.

[19] Marcum, D. L., "Advancing-Front/Local-Reconnection (AFLR) Unstructured Grid Generation," *Computational Fluid Dynamics Review*, World Scientific, Singapore, 1998, p. 140.